Chem. Senses 28: 113–130, 2003

Projections to Higher Olfactory Centers from Subdivisions of the Antennal Lobe Macroglomerular Complex of the Male Silkmoth

Ryohei Kanzaki, Kajin Soo, Yoichi Seki and Satoshi Wada

Institute of Biological Sciences, University of Tsukuba, 1-1-1 Tsukuba, Ibaraki 305-8572, Japan

Correspondence to be sent to: Ryohei Kanzaki, Institute of Biological Sciences, University of Tsukuba, Tsukuba, Ibaraki 305-8572, Japan. e-mail: kanzaki@biol.tsukuba.ac.jp

Abstract

The macroglomerular complex (MGC) is the first-order center for synaptic processing of olfactory information about the female sex pheromone in the male moth brain. We have investigated the MGC subdivisions of the male silkmoth *Bombyx mori* by use of three-dimensional reconstruction of the MGC from sequential series of confocal slice images. The *B. mori* MGC consists of three subdivisions similar to those of *Manduca sexta*: the cumulus, toroid and horseshoe. Intracellular recording and staining revealed that responses of MGC projection neurons to pheromonal stimulation correlate with their dendritic arborizations in the subdivisions of the MGC (the cumulus, toroid and horseshoe) and each subdivision specific projection neuron transmits information to different regions in the calyces of the mushroom body and the inferior lateral protocerebrum. We revealed that major pheromone component information is transferred to the medial part of the inferior lateral protocerebrum through three different antennocerebral pathways. Although it is generally accepted that the calyces of the mushroom body and the inferior lateral protocerebrum are the target sites for pheromone information from the MGC in moths, our results suggest that the medial part of the inferior lateral protocerebrum may be a more important processing site for major pheromonal information in *B. mori*.

Key words: brain, insect, mushroom body, pheromone, three-dimensional reconstruction

Introduction

Due to the anatomical similarity of the primary olfactory centers of diverse animals, such as the antennal lobes (ALs) of insects and the olfactory bulbs of vertebrates, the insect ALs have been popular models for the study of olfactory processing (Hildebrand and Shepherd, 1997; Christensen and White, 2000).

Male silkmoths (*Bombyx mori*) exhibit a characteristic zigzagging pattern as they walk upwind toward pheromones released by conspecific females (Kanzaki, 1998). The female sex-pheromone blend contains two components. The major component (*E*,*Z*)-10,12-hexadecadienol (bombykol) is sufficient to trigger the complete mating behavior. Conversely, the minor component (*E*,*Z*)-10,12-hexadecadienal (bombykal) is known to have an inhibitory effect on the mating behavior (Kaissling and Kasang, 1978). It has been reported that silkmoth female glands contain bombykol and bombykal in a ratio of 9:1 (Kaissling and Kasang, 1978). Morphologically the antennae of male *B. mori* have slightly longer flagellar branches and a greater number of sensory hairs (sensilla trichodea) than the female (i.e. they are sexually dimorphic). The antennae of the male *B. mori* have ~17 000 trichodial hairs, each of which contains two types of olfactory receptor neurons (ORNs), each sensitive to one of the two components (Kaissling and Priesner, 1970; Kaissling and Kasang, 1978).

These ORNs send axons into the first order olfactory center, the ALs where they make synapses with postsynaptic neurons in conspicuously arranged rounded modules known as glomeruli (Kanzaki and Shibuya, 1986; Koontz and Schneider, 1987). The male *B. mori* AL comprises ~57 ordinary glomeruli (Gs) and sexually dimorphic glomeruli called the macroglomerular complex (MGC) (Kanzaki and Shibuya, 1983, 1986; Soo and Kanzaki, 2000). The MGC is the first-order center for synaptic processing of olfactory information about the female sex pheromone in the male moth brain (Boeckh and Boeckh, 1979; Matsumoto and Hildebrand, 1981; Kanzaki and Shibuya, 1986; Christensen and Hildebrand, 1987). Koontz and Schneider (Koontz and Schneider, 1987) reported that the *B. mori* MGC is subdivided into four compartments, each compartment consisting of one or more glomeruli surrounding a central core of neuropil (MGC 1, 2, 3, 4). In the hawkmoth (*Manduca sexta*), the largest MGC glomerulus is situated closest to the entrance of the antennal nerve and is named the 'cumulus', a second, doughnut-shaped MGC glomerulus is called the 'toroid' and a third subunit is named the

'horseshoe' (Strausfeld, 1989; Hansson *et al.*, 1991; Heinbockel *et al.*, 1998).

Intracellular recording has been invaluable in deciphering the coding mechanisms used by AL local interneurons (LNs) and projection neurons (PNs, AL output neurons) (Matsumoto and Hildebrand, 1981; Kanzaki and Shibuya, 1986; Christensen and Hildebrand, 1987, 1996; Kanzaki *et al.*, 1989; Hildebrand, 1996; Hansson and Christensen, 1999). *M. sexta* PNs that innervate the cumulus respond selectively to the minor pheromone component, while those innervating the toroid respond selectively to the major component (Hansson *et al.*, 1991). Numerical comparison of cells in the ALs of *M. sexta* males and females using anatomical techniques has demonstrated that the males have about 30 MGC-PNs (Homberg *et al.*, 1988).

In some species of moths, the number of MGC compartments in the male AL corresponds to the number of pheromone components to which the species' olfactory receptor neurons respond, while in other moth species the number of the MGC compartments is smaller (Vickers *et al.*, 1998; Hansson and Christensen, 1999). The functional subdivisions in the MGC have been well studied neurophysiologically in several species of moths (Hansson *et al.*, 1991; Hansson and Christensen, 1999). However, the projection sites in higher olfactory centers in the protocerebrum (PC) from each subdivision are still unclear.

In the present study we investigated the MGC subdivisions of the male *B. mori* by use of three-dimensional (3-D) reconstruction of the MGC from sequential series of confocal slice images. Morphological and physiological properties of PNs which have arborizations in each subdivision of the MGC were investigated. We found that the *B. mori* MGC consists of three subdivisions similar to those of *M. sexta*: the cumulus, toroid and horseshoe. Here we demonstrate that subdivision specific projection neurons transmit information about functionally different pheromone components through three different antennocerebral pathways to different regions in higher olfactory centers, the calyces of the mushroom body (Ca) and the inferior lateral protocerebrum (ILPC). Response patterns of MGC-PNs to pheromonal stimuli correlate with their dendritic arborizations in the subdivisions of the MGC. Also, we demonstrate that the ILPC may be a more important processing site than the Ca for major pheromonal information in *B. mori*.

Materials and methods

Physiology

Bombyx mori (Lepidoptera: Bombycidae) were reared on an artificial diet at 26°C and 60% relative humidity. Methods employed in this study have been described elsewhere (Kanzaki and Shibuya, 1986; Kanzaki *et al.*, 1989; Mishima and Kanzaki, 1999). Adult male moths were used 3–6 days following eclosion. After cooling (4°C, ~30 min) to achieve anesthesia, the intact moth with its ventral side down was waxed to a plastic chamber. The head was immobilized with a notched plastic yoke slipped between the head and thorax. Wings and legs were also immobilized in the chamber. The brain was exposed by opening the head capsule and removing large tracheae; intracranial muscles were removed to eliminate brain movements. The antennal lobe was surgically desheathed to facilitate insertion of microelectrodes. Electrodes were filled with 4% Lucifer Yellow CH (LY) solution (Sigma, St Louis, MO) in distilled water. The resistance of the electrodes was ~100 MΩ. A silver ground electrode was placed in the body. The brain was superfused with saline solution (mM): 140 NaCl; 5 KCl; 7 $CaCl_2$; 1 $MgCl_2$; 4 $NaHCO_3$; 5 trehalose; 5 *N*-tris (hydroxymethyl) methyl-2-aminoethanesulfonic acid (TES); and 100 sucrose (pH 7.3). Electrical responses of AL neurons were monitored with an oscilloscope and recorded on a DAT recorder (RD-125T; TEAC, Tokyo, Japan) at 24 kHz. The acquired signals were stored on a computer through an A/D converter (Quik Vu II; TEAC, Tokyo, Japan). The voltage level of the baseline was set above the noise voltage level. The number of impulses above the baseline was measured and processed by the computer and shown as impulse-frequency histograms (0.2 s bins).

Olfactory stimulation

Three olfactory stimuli were used in these experiments: (i) bombykol (*E*10,*Z*12–16:AL; primary pheromone component) (Butenandt *et al.*, 1949); (ii) bombykal (*E*10, *Z*12–16:OH; minor pheromone component) (Kaissling and Kasang, 1978); and (iii) 1-hexanol (E6:AL; a leaf odor). Air-puff stimuli similar to those described previously (Kanzaki *et al.*, 1994) were used. Odorants were applied to a piece of filter paper (1 × 1 cm) as a 5 µl solution and then inserted into a glass stimulant cartridge (Pasteur pipette, 1 mm tip diameter). Odor concentration is expressed as the amount of stimulant applied to the filter paper. In the present study 10 ng bombykol, 10 ng bombykal and 5 µl hexanol were used. Since the female gland is known to contain bombykol and bombykal in a ratio of 9:1, 9 ng bombykol + 1 ng bombykal were used as blend stimulation (Kaissling and Kasang, 1978). Olfactory stimulation was applied to the antenna ipsilateral to the AL. Each stimulus was a 500 ms puff at a velocity of ~17.5 cm/s and the interval between puffs was at least 30 s.

3-D reconstruction of a single neuron

We stained each neuron by iontophoretic injection of LY with constant hyperpolarizing current (–1 nA) for 5–10 min. The brain was fixed in 4% paraformaldehyde in 0.2 M phosphate buffer (pH 7.4) for 1 h at room temperature and dehydrated with an ethanol series and cleared in methyl salicylate. Each stained neuron was imaged frontally using a confocal imaging system (LSM-510; Carl Zeiss, Jena, Germany) with plan apochromat ×20 (n.a. = 0.75) and ×40 (n.a. = 1.0) objectives. The LY-stained neurons were

examined with 458 nm excitation and a long-pass emission filter (>475 nm) in whole mount. In cases where the subdivisions of the MGC were unclear, the brain was immersed in Alexa Fluor 568 (Molecular Probes Europe BV) for 1 h for background staining. The background was examined with 543 nm excitation and a long-pass emission filter (>560 nm) in whole mount. Serial optical sections were acquired at 0.7 μm intervals throughout the entire depth of a neuron. 3-D reconstructions of the labeled neurons were made from these sections.

3-D reconstruction of the MGC

The dissected brains were prefixed in 4% paraformaldehyde in 0.2 M phosphate buffer (pH 7.4) for 2 min and immersed in 0.1% LY solution for 4 h at room temperature. The brains were then fixed in 4% formaldehyde for 1 h at room temperature and dehydrated with an ethanol series and cleared in methyl salicylate. Each stained brain was imaged frontally using a confocal imaging system with a plan apochromat ×40 (n.a. = 1.0) objective. Serial optical slices were acquired at 0.7 μm intervals. These images were read into an image processing software (Amira; TGS, Berlin, Germany) and analyzed. MGCs which were traced in each optical slice were three-dimensionally reconstructed.

Results

Subdivisions of the *B. mori* MGC

As with males of many other species of moths, the AL of the male *B. mori* consists of coarse neuropil and a specific number of spheroidal neuropil compartments called glomeruli. According to the shape, position and size, two types of glomeruli were characterized (Figure 1A). A male specific macroglomerular complex (MGC; diameter 150–200 μm) exists at the entrance of the AL and ~57 small-sized glomeruli (ordinary glomeruli, diameter 30–50 μm) exist ventro-medial to the MGC and are arranged surrounding the coarse neuropil (Soo and Kanzaki, 2000).

As shown in Figure 1A, the MGC consists of three subdivisions. To know the detailed structure of these sub-

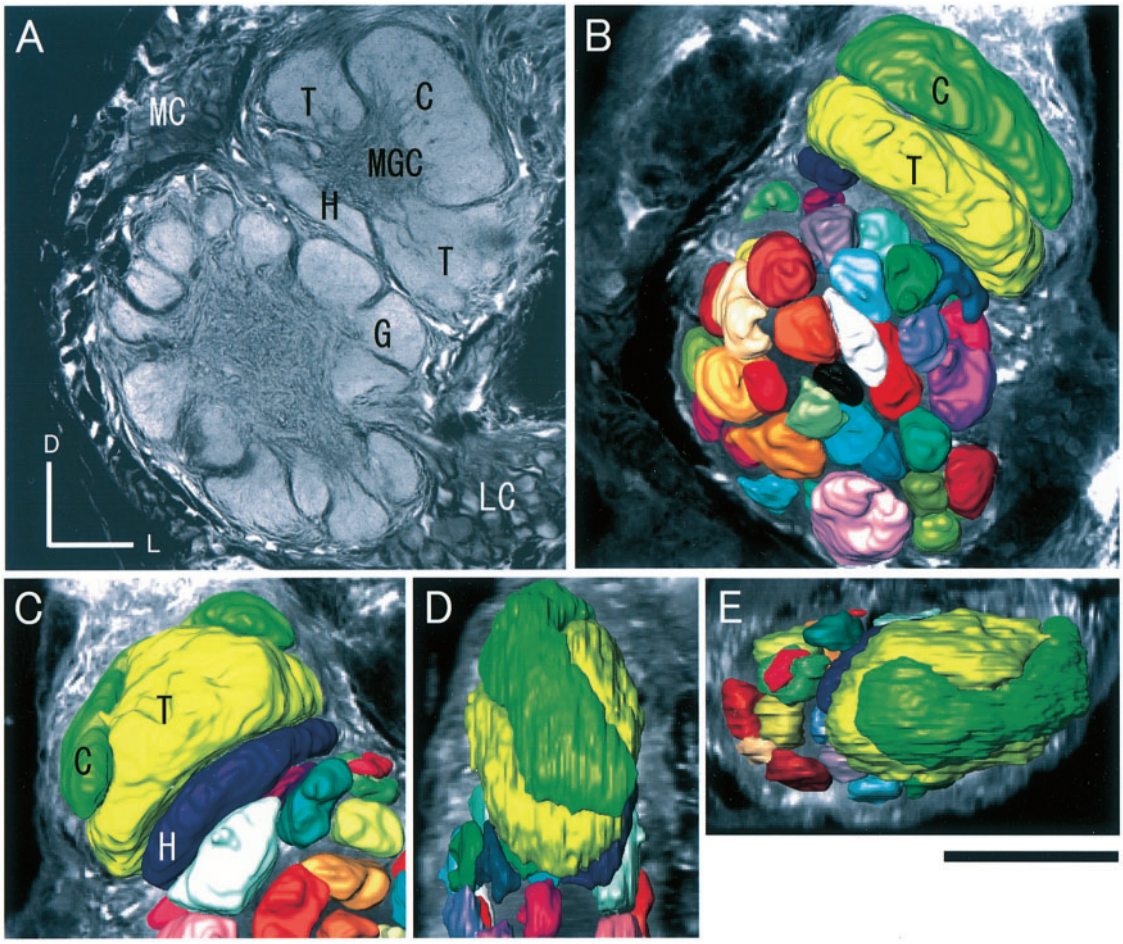

Figure 1 Antennal lobe of the male silkworm moth, *Bombyx mori*. **(A)** A confocal slice image of the LY-stained AL. Three prominent subdivisions of the MGC, the cumulus (C), toroid (T) and horseshoe (H) are shown. **(B–E)** 3-D reconstruction of the MGC from four different views are shown. Frontal view **(B)**, posterior view **(C)**, side view **(D)**, and dorsal view **(E)**. Scale bar = 100 μm. Direction: D, dorsal; L, lateral.

divisions 3-D reconstructions of the MGC were made from series confocal slice images (Figure 1B–E). Three distinct subdivisions were easily observed. These are: a globular region situated at the entrance of the AL; a doughnut-shaped region of neuropil adjacent to the globular region; and a small neuropil ventral to the doughnut-shaped region. These subdivisions correspond to the 'cumulus', 'toroid' and 'horseshoe' MGC subdivisions described in *M. sexta* (Strausfeld, 1989; Hansson *et al.*, 1991). Koontz and Schneider (Koontz and Schneider, 1987) reported that the MGC of the male *B. mori* is subdivided into compartments consisting of a central glomerulus (MGC 1) and three ring-shaped glomeruli (MGC 2, 3, 4). The MGC 2, 3 and 4 correspond to the cumulus, toroid and horseshoe, respectively. 3-D reconstruction of the MGC revealed that the MGC 1 is a protuberant part of the toroid (MGC 3) rising dorsally into the cumulus (MGC 2) from a posterior part of the toroid (Figures 1C, 8).

While slight variations in the form of the subdivisions of the MGC were observed in different individuals (n = 11), subdivisions into three compartments appeared to be a constant feature. Here we use the nomenclature of these subdivisions according to those of *M. sexta* (Strausfeld, 1989; Hansson *et al.*, 1991)

MGC-projection neurons

Thirty-seven MGC-projection neurons (PNs) were three-dimensionally characterized by intracellular staining with LY (Table 1). Olfactory responses were recorded from 14 out of 37 MGC-PNs. Thirty-one out of 37 MGC-PNs had their cell bodies in the medial cell group (MC) in the AL. Twenty-nine out of 31 had axons running in the inner antennocerebral tract (IACT) leading to the protocerebrum, including the calyces of the mushroom body (Ca) and the inferior lateral protocerebrum (ILPC). Two out of 31 had axons in the IACT leading to the ILPC, but not to the Ca. Six MGC-PNs had their cell bodies in the lateral cell group (LC) in the AL. The axons were in the medial antennocerebral tract (MACT, n = 3) or the outer antennocerebral tract (OACT, n = 3) and sent terminal branches exclusively to the ILPC. None of these PNs projected to the Ca (Table 1). According to the branching areas of dendritic arborizations in the subdivisions of the MGC, MGC-PNs characterized in this study were classified into the following four groups (Table 1).

Cumulus-PNs

Morphology

Nine PNs were classified into this group (Table 1). In all of these PNs, dendritic arborizations were restricted to the cumulus. Dendritic arborizations of most of the cumulus-PNs appeared to be uniformly distributed throughout the cumulus with numerous fine spines (Figures 2 and 3). A few cumulus-PNs had arborizations separated into some distinct tufts in partitions similar to those of the toroid-PNs (data not shown).

The cumulus-PN cell bodies (diameter 10–15 μm) resided in the MC of the AL and the axons passed through the IACT to the Ca and ILPC (Figures 2 and 4 and Table 1). The axons of the PNs sent some blebby axonal branches into the whole calyces and extended blebby terminals into the ILPC (Figures 2 and 4). Small-field branches were restricted to the lateral part of the ILPC (Figure 4).

Physiology

Olfactory responses were recorded from five out of nine PNs in this group. One example is shown in Figure 5. The morphology of this cell is shown in Figure 3E. This PN showed strong excitatory responses to bombykal and pheromone blend applied to the ipsilateral antenna, whereas no responses were elicited by bombykol, hexanol or clean air stimulus (control). The background activity was <2 Hz. The peak firing frequency evoked by bombykal was ~85 Hz. The initial period of phasic firing with a membrane depolarization was followed by a reduction in spike frequency. The

Table 1 Morphological properties of MGC-projection neurons

	Cumulus-PNs	Toroid-PNs		c + t-PNs		Horseshoe-PNs
Branching areas of dendritic arborizations	cumulus	toroid[a]		cumulus and toroid[b]		horseshoe[c]
Position of the cell body	MC	MC		LC		MC
Axon paths to PC	IACT	IACT		MACT	OACT	IACT
Projection region in PC	Ca L-ILPC	(Ca)[d] + M-ILPC	M-ILPC	M-ILPC	M-ILPC	Ca L-ILPC
n	9	15	2	3	3	5

L-ILPC, lateral part of the ILPC; M-ILPC, medial part of the ILPC.

[a]One toroid-PN had a few thin processes with blebs projecting into the cumulus (Figure 8A, arrows).

[b]One c + t-PN had arborizations in the horseshoe (Figure 13C).

[c]One horseshoe-PN had branchings partly in the toroid (data not shown).

[d]Only a single or a few short blebby branches into the Ca (Figure 9A).

membrane potential was hyperpolarized and firing was suppressed for ~2.5s before restoration of the normal background firing rate. Another two sets of olfactory stimulation consistently elicited similar response patterns.

Spike frequency histograms of four cumulus-PNs are shown in Figure 6. Cell 1 (top row) of the histograms are of the PN shown in Figure 5. All of these PNs showed excitatory responses to bombykal and the pheromone blend. No response was elicited by bombykol, hexanol or control in the cumulus-PNs tested. Thus, the cumulus-PNs tested in this study responded exclusively to the minor pheromone component, bombykal.

Toroid-PNs

Morphology

Seventeen PNs were classified into this group (Table 1). Fifteen out of 17 toroid-PNs had dendritic arborizations separated into some distinct tufts in the toroid subdivisions (Figures 7A and 8A–D). A variety of distinct tufts in partitions were observed. In one toroid-PN a few thin processes with fine blebs were observed projecting into the cumulus (arrows in Figure 8A). The toroid-PNs had branchings with tufts in the medio-dorsal part of the MGC (Figure 8A–8D, thick arrows). This region is a protuberant structure rising dorsally into the cumulus from a posterior part of the toroid (Figure 1C). Two out of 17 toroid-PNs had dendritic arborizations with numerous fine spines, similar to those of the cumulus-PNs (Figures 7B and 8E,F). In case of the PN shown in Figure 8E, arborizations were restricted to a distinct partition, the lateral posterior part of the toroid.

All the toroid-PN cell bodies (diameter 10–15 μm) resided in the MC of the AL and the axons passed through the IACT (Table 1). Fifteen out of 17 toroid-PNs sent only a single or a few short blebby branches into the Ca (Figures 7A and arrows in Figure 9A). In contrast, wide-field branches with thick blebs were consistently observed in the medial part of the ILPC (Figure 9). Two toroid-PNs which had dendritic arborizations with numerous fine spines sent wide-field thick blebby branches extending into the medial part of the ILPC bypassing the Ca (Figure 7B).

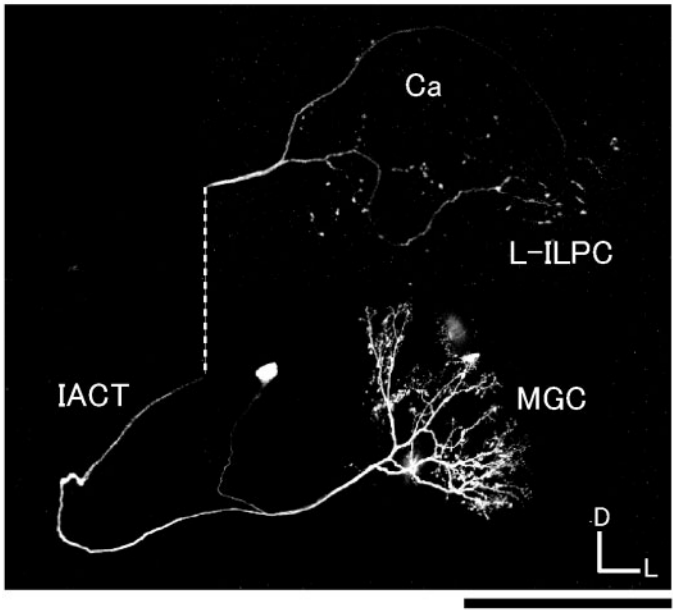

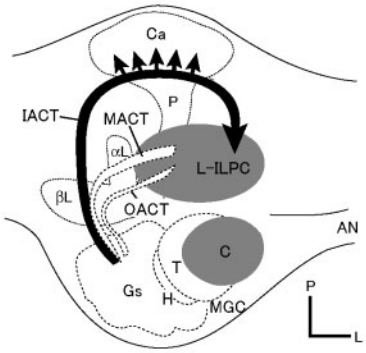

Figure 2 Morphology of a cumulus-PN, Frontal view. Confocal slice image is shown in Figure 3A. Dendritic arborizations are restricted to the cumulus. The cell body is in the MC. The axon runs in the IACT and sends blebby branchings to the Ca and the lateral part of the ILPC (L-ILPC). The dashed line links processes that were separated to reveal the structures of branches that overlapped *in situ*. Scale bar = 100 μm. Inset is a schematic drawing of the hemisphere of the brain showing projection sites of the cell. The IACT, MACT and OACT run ventral to the lobes of the MB. Direction: L, lateral; P, posterior.

Physiology

Olfactory responses were recorded from 8 out of 17 toroid-PNs. One example is shown in Figure 10. The morphology of this cell is shown in Figure 7B. This toroid-PN showed strong excitatory responses with membrane depolarization to bombykol and the pheromone blend applied to the ipsilateral antenna, whereas no responses were elicited by bombykal, hexanol or clean air. Membrane depolarization gave rise to a train of spikes and the firing was suppressed for ~1s before restoration to the normal background firing rate. The background activity was <5 Hz. The peak firing frequency evoked by bombykol was ~80 Hz. Another two sets of olfactory stimulation showed similar response patterns.

Another example is shown in Figure 11. The morphology of this cell is shown in Figure 7A. This toroid-PN also showed strong excitatory responses to bombykol and the pheromone blend. Moreover, inhibitory responses with membrane hyperpolarizations were elicited by bombykal. No responses were elicited by hexanol or control. The background activity was <10 Hz. The peak firing frequency evoked by bombykol was ~75 Hz. Another two sets of olfactory stimulation showed similar response patterns.

Olfactory responses of seven toroid-PNs are shown as

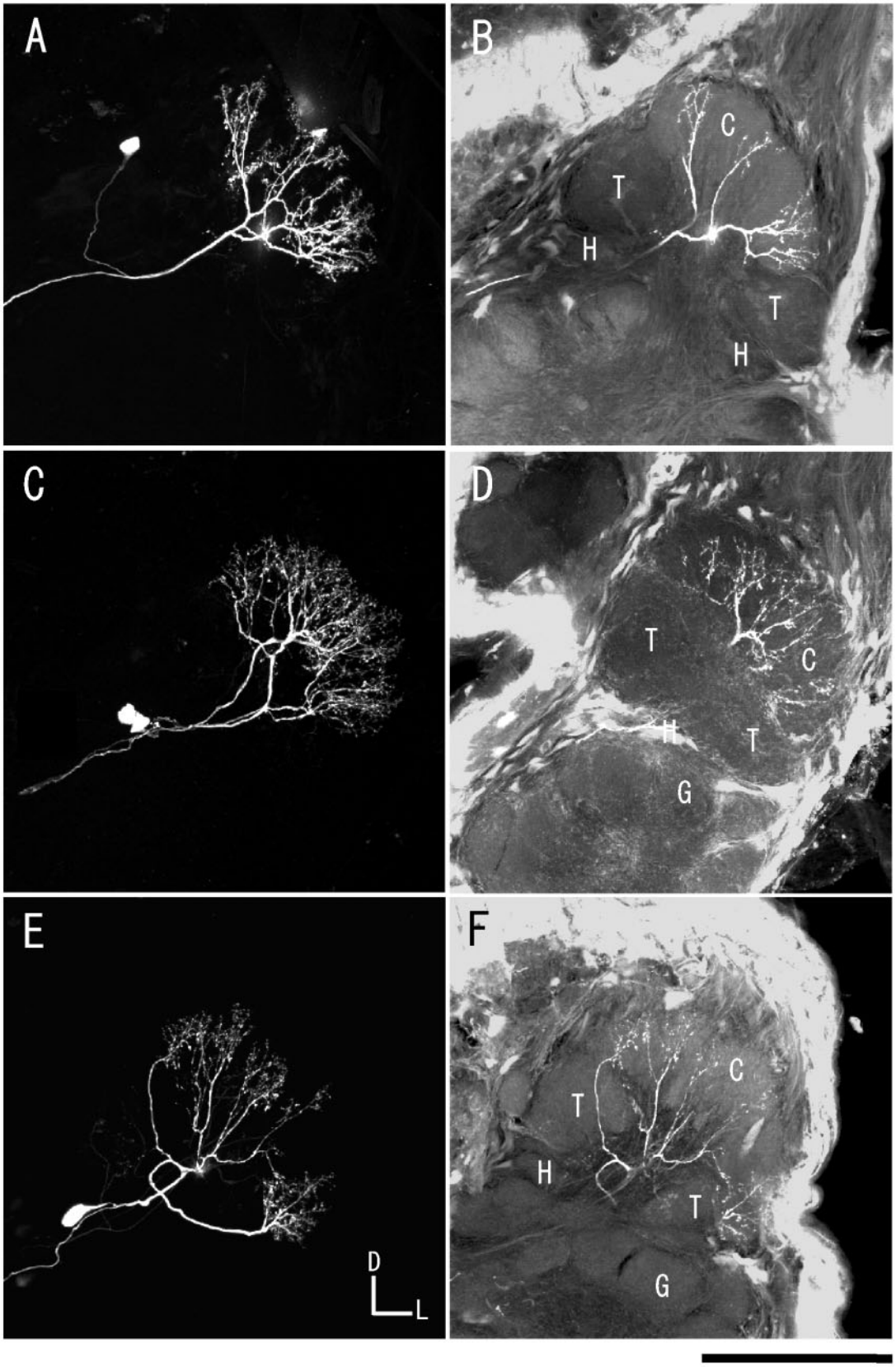

Figure 3 Dendritic arborizations of cumulus-PNs in the MGC. **(A, C, E)** Dendritic branches of three different cumulus-PNs. Frontal view. **(B, D, F)** B, D and F are confocal slice sections of A, C and E, respectively. Branching regions of each of the PNs are restricted to the cumulus (C). All PNs have cell bodies in the MC. Scale bar = 100 μm.

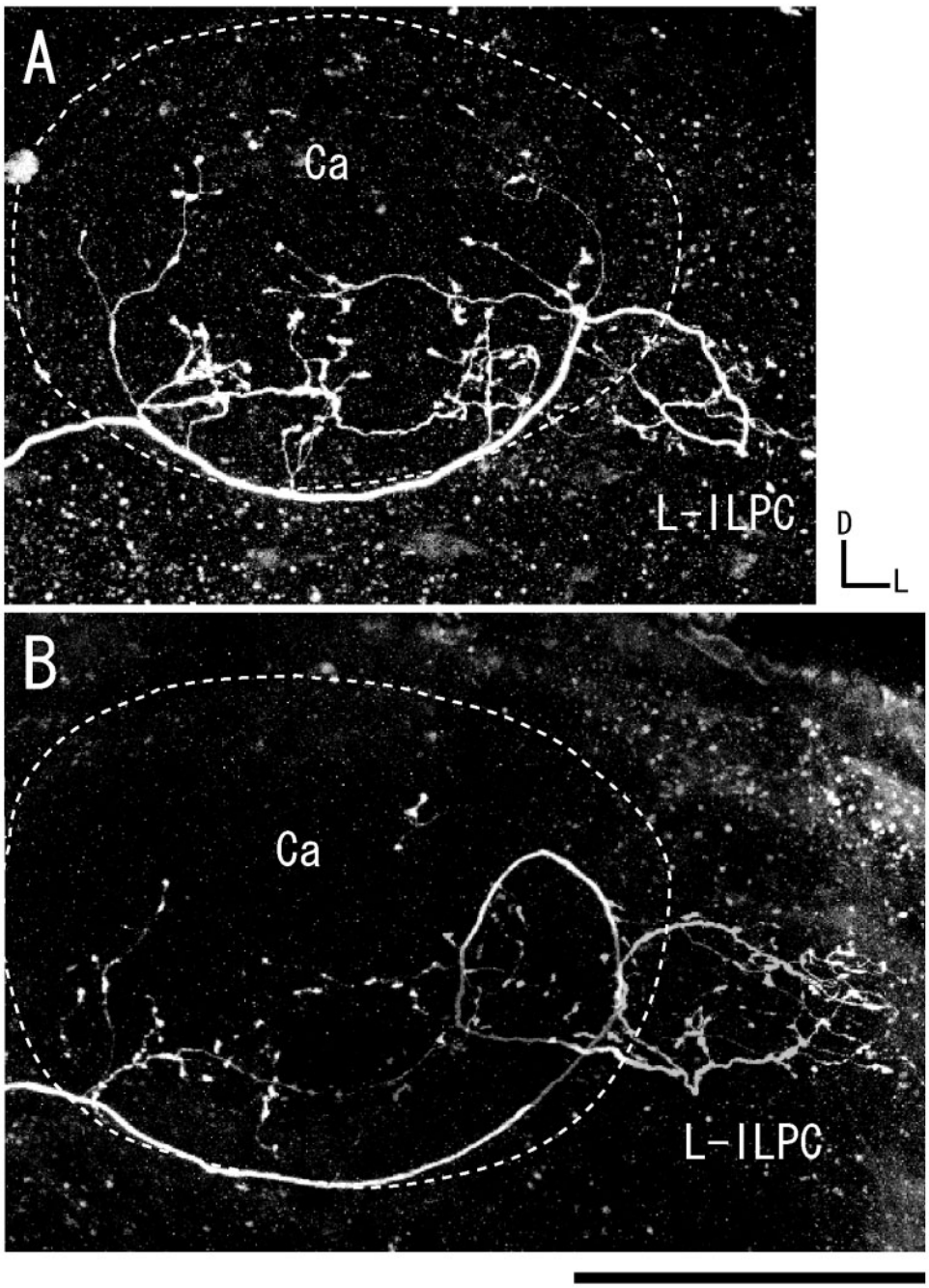

Figure 4 Morphology of cumulus-PNs in the protocerebrum. **(A, B)** Axons of both cumulus-PNs pass through the IACT and send blebby axonal branches into the whole calyces and extend blebby terminals into the lateral part of the ILPC (L-ILPC). Scale bar = 100 μm.

spike-frequency histograms in Figure 12; cells 2 and 3 are of the PNs shown in Figures 10 and 11, respectively. All of these toroid-PNs showed excitatory responses selectively to bombykol. In the present study six out of eight toroid-PNs showed excitatory responses to bombykol and no response to bombykal, while two out of eight toroid-PNs showed excitatory responses to bombykol and inhibitory responses to bombykal. None of the eight toroid-PNs tested responded to hexanol or control. Thus, the toroid-PNs tested in this study showed excitatory responses selectively to the major component of the pheromone, bombykol.

Cumulus and toroid-PNs (c + t-PNs)

Morphology

Six PNs were classified into this group (Table 1). All these c + t-PNs had a major neurite extending into two or three subdivisions of the MGC. Each of the neurites gave rise to

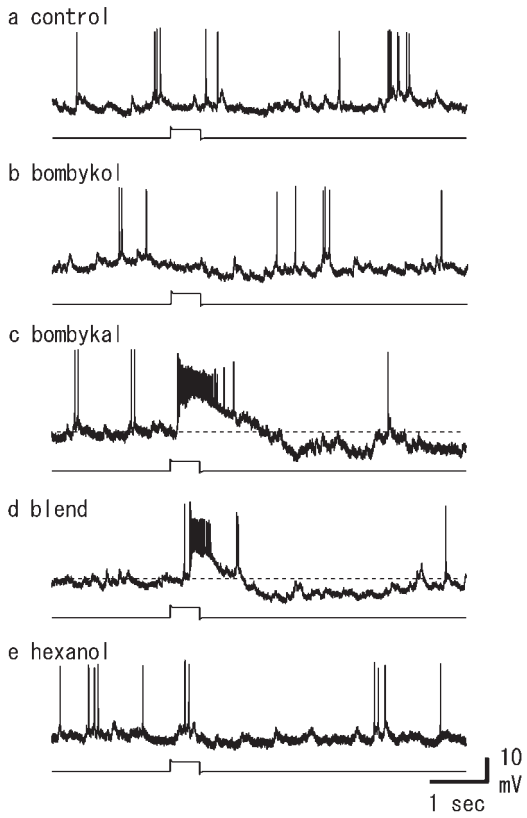

Figure 5 Physiological profile of the cumulus-PN shown in Figure 3E. Responses to antennal stimulation with two pheromone components and leaf odor (hexanol). The cell showed excitatory responses selectively to bombykal and blend. Bombykol, hexanol and control did not elicit any responses. Another two sets of olfactory stimulation showed similar response patterns.

numerous filamentous branches with fine spines throughout the whole MGC including the cumulus and toroid (Figure 13). One c + t-PN had fine branches in the horseshoe as well (arrows in Figure 13C). The cell bodies (diameter 10–15 μm) of these PNs resided in the LC of the AL. Only the PNs classified into this group had their cell bodies in the LC (Table 1). The axons passed through the medial antennocerebral tract (MACT, n = 3) or the outer antennocerebral tract (OACT, n = 3) to the ILPC. The axons sent wide-field blebby branches into the medial part of the ILPC. No projections were observed in the Ca (Figure 13A,D and Table 1). Although the paths to the PC are different, i.e. MACT or OACT, it seems that the projection areas of these two types of c + t-PNs overlap in the ILPC (Figure 13D).

Physiology

Olfactory responses were recorded from one out of six c + t-PNs. Olfactory responses of this cell are shown in Figure 14. The morphology of the cell is not shown because of weak staining of the cell. However, the morphological characteristics were similar to those of the PN shown in Figure 13A. This c + t-PN showed strong excitatory responses with membrane depolarization to bombykol, bombykal and the pheromone blend. Weak excitation was also recorded in response to control and hexanol, suggesting a weak mechanosensory response. The background activity was <2 Hz. The peak firing frequencies evoked by bombykol and bombykal were ~75 and ~65 Hz, respectively. Another two sets of olfactory stimulation showed similar response patterns.

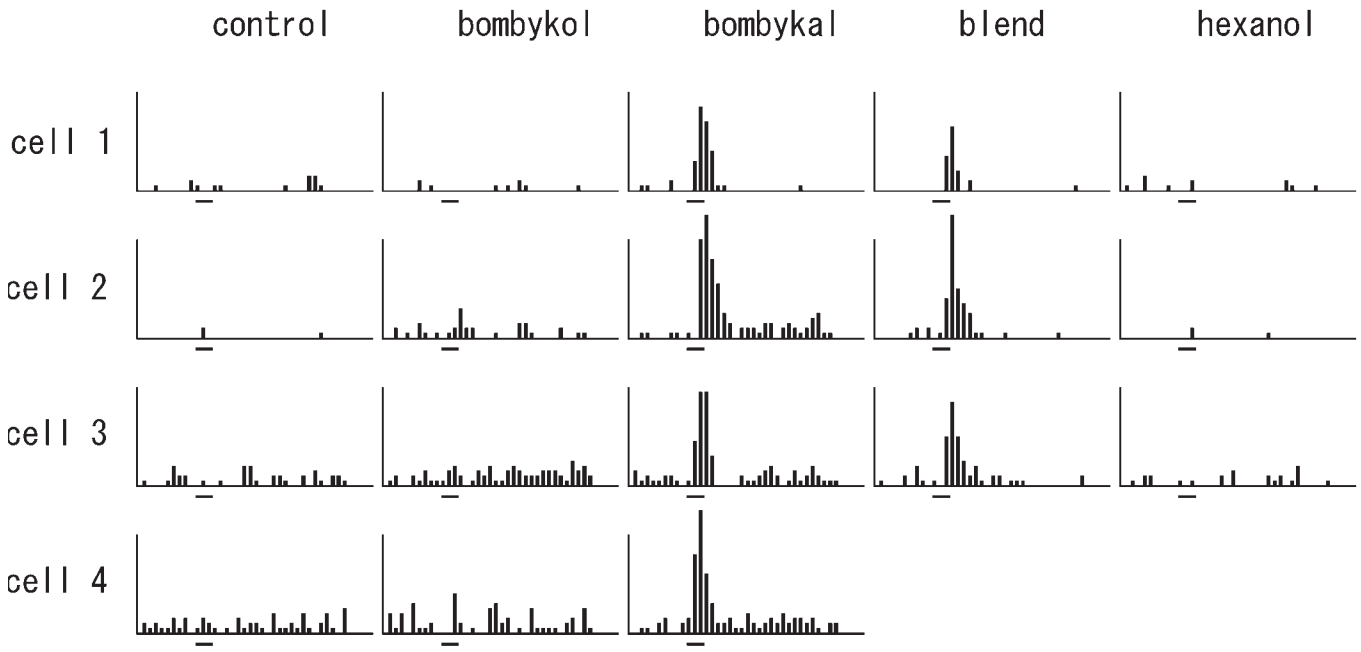

Figure 6 Spike frequency histograms for cumulus-PNs. All the cumulus-PNs tested selectively responded to bombykol and blend with excitation; x-axis = 0–7 s; stimulus marker = 0.5 s; y-axis = 0–20 spikes/0.2 s bin.

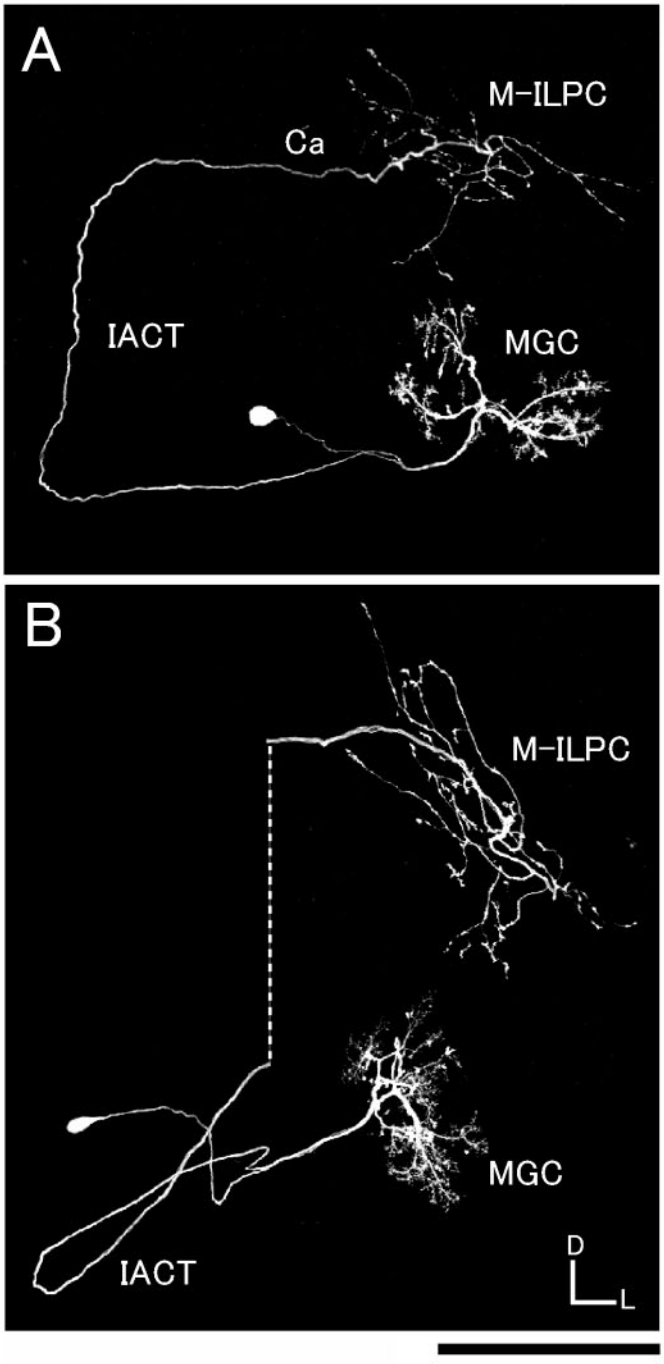

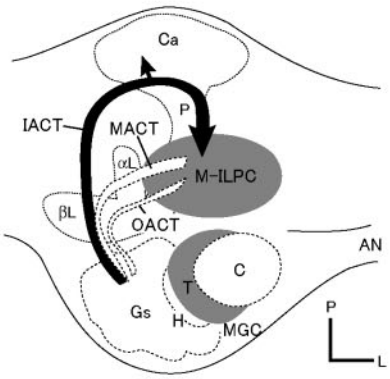

Horseshoe-PN

Morphology

Five PNs were classified into this group (Table 1). Four out of five PNs had dendritic arborizations with numerous fine spines restricted to the horseshoe (Figure 15B). One out of five horseshoe-PNs had arborizations mainly in the horseshoe and partly in the toroid (data not shown). All horseshoe-PNs had cell bodies (diameter 10 μm) in the MC of the AL. The axons of the PNs passed through the IACT to the Ca and ILPC (Table 1). The axons sent some blebby branches into the medio-ventral part of the Ca and into the lateral part of the ILPC with small-field blebby branchings (Figure 15A).

Physiology

Olfactory responses were recorded from one out of five horseshoe-PNs. Olfactory responses of this cell are shown in Figure 16. Morphological characteristics of the cell were similar to those of the horseshoe-PN shown in Figure 15. This horseshoe-PN showed excitatory responses with membrane depolarization to bombykal applied to the ipsilateral antenna, whereas no responses were elicited by bombykol, mixture, hexanol or clean air. Although bombykal (10 ng) elicited excitatory responses, the mixture which contained 1 ng bombykal did not excite the PN. This might be caused by low concentration (sub-threshold) of bombykal stimulation or perhaps mixture suppression. The background activity was <5 Hz. The peak firing frequency evoked by bombykal was ~50 Hz. Another two sets of olfactory stimulation showed similar response patterns.

Discussion

Subdivisions of the MGC

Initial sex-pheromone processing in the insect brain takes place in the male-specific MGC of the AL (Boeckh and Tolbert, 1993; Christensen and Hildebrand, 1996; Hildebrand, 1996; Christensen and White, 2000). It has also been reported that the MGC consists of several functional subdivisions in *M. sexta* and *Heliothis virescens* (Hansson *et al.*, 1991; Vickers *et al.*, 1998). Koontz and Schneider (Koontz and Schneider, 1987) reported that the MGC of the male *B. mori* is subdivided into four compartments consisting of a central glomerulus (MGC 1) and three

Figure 7 Morphology of toroid-PNs. **(A)** This cell has dendritic arborizations separated into some distinct tufts in the toroid and a cell body in the MC. The axon passes through the IACT and sends only a single or a few short blebby branches into the ventro-anterior part of the Ca and wide-field terminals with dense blebs into the medial part of the ILPC (M-ILPC). **(B)** This cell has dendritic arborizations with numerous fine spines. Arborizations were restricted to a distinct partition, the lateral posterior part of the toroid. The axon runs in the IACT and sends blebby terminals extending to the M-ILPC. No branches were observed in the Ca. Scale bar = 100 μm. Inset is a schematic drawing of the hemisphere of the brain showing projection sites of the cell.

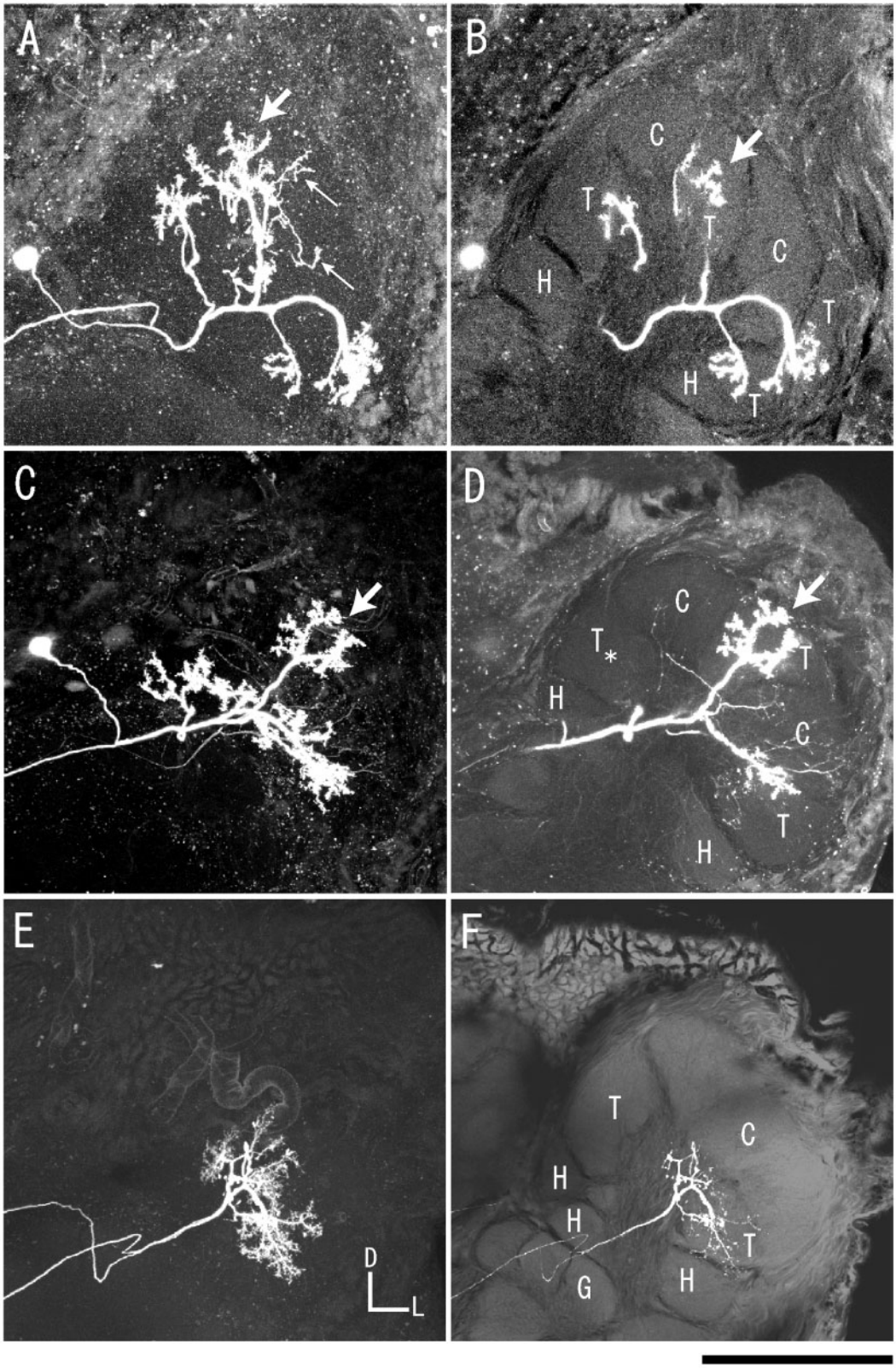

Figure 8 Dendritic arborizations of toroid-PNs. **(A, C, E)** Dendritic branches of three different toroid-PNs. Frontal view. **(B, D, F)** B, D and F are the confocal slice sections corresponding to A, C and E, respectively. Branching regions of each of the PNs are restricted to the toroid (T). Asterisks in D: tufted branches in the marked part of the toroid are not visible in this section. All PNs have their cell bodies in the MC. Arrows in A: a few thin processes with fine blebs were observed projecting into the cumulus. Thick arrows in A–D: a protuberant structure rising dorsally into the cumulus from a posterior part of the toroid. Scale bar = 100 μm.

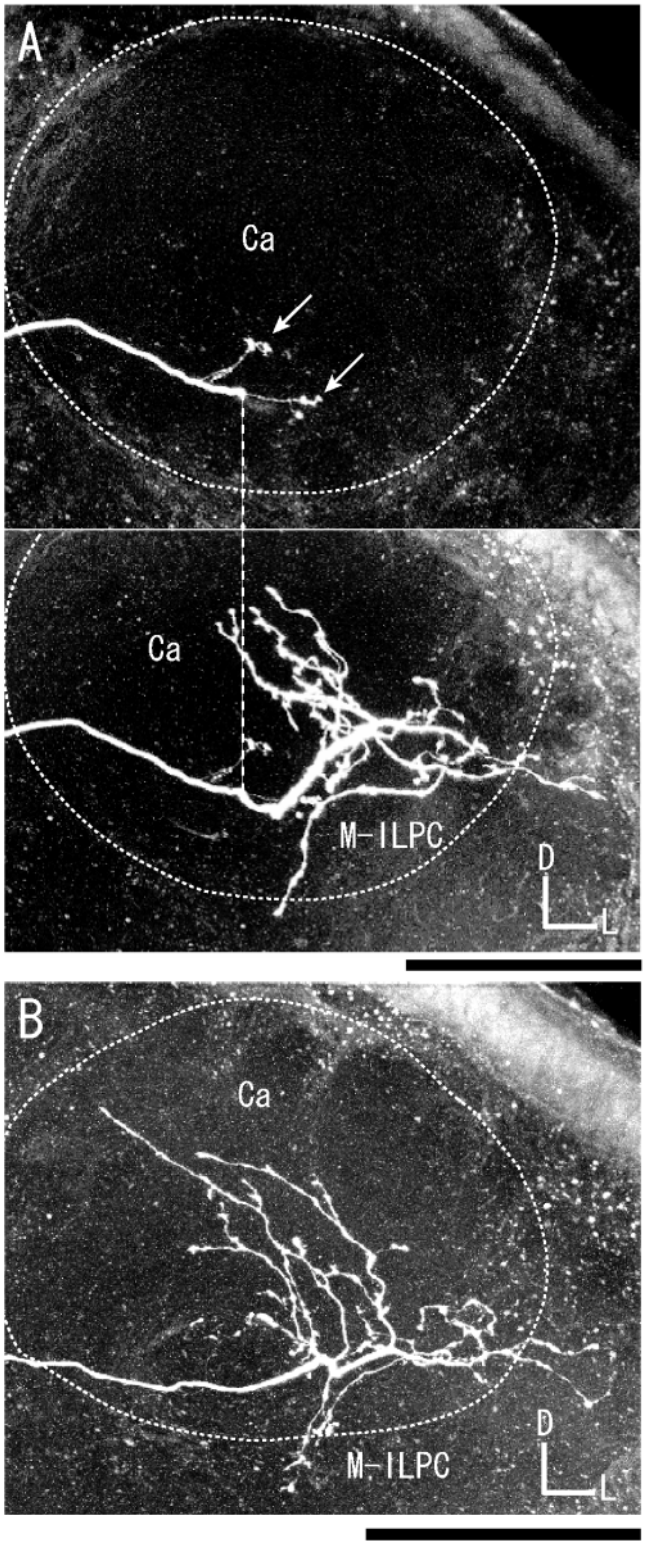

Figure 9 Morphology of toroid-PNs in the protocerebrum. **(A, B)** Similar to the toroid-PN shown in Figure 7A, axons of both toroid-PNs pass through the IACT and send only a single or a few short blebby branches into the ventro-anterior part of the Ca (arrows) and the medial part of the ILPC (M-ILPC) with wide-field terminals with dense blebs. The dashed line links processes that were separated to reveal the structures of branches that overlapped *in situ*. Scale bar = 100 μm.

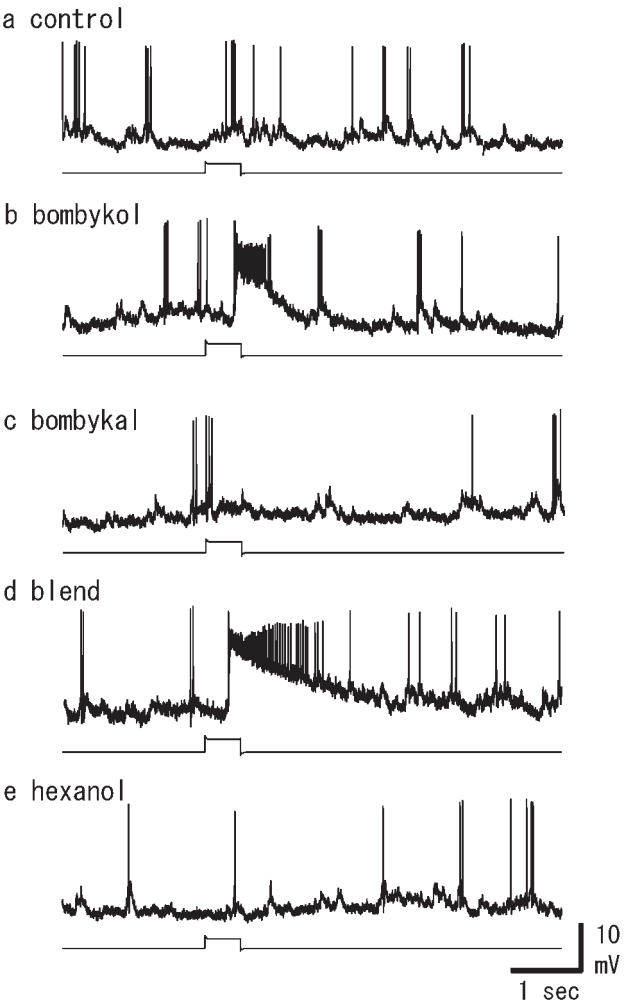

Figure 10 Physiological profile of the toroid-PN shown in Figure 7B. Responses to antennal stimulation with two pheromone components and hexanol. The cell showed excitatory responses selectively to bombykol and blend. Bombykal, hexanol and control did not elicit any responses. Another two sets of olfactory stimulation showed similar response patterns.

ring-shaped glomeruli (MGC 2, 3, 4). In the present study 3-D reconstruction of the *B. mori* MGC has led to some important advances in understanding the structure of the MGC. Our results revealed that MGC 2, 3 and 4 correspond to the cumulus, toroid and horseshoe, respectively. The structure of the *B. mori* MGC is fundamentally similar to that of *M. sexta* (Hansson *et al.*, 1991); however, some different structures were observed. That is, Koontz and Schneider (Koontz and Schneider, 1987) reported that MGC 1 is a central glomerulus independent from the other ring-shaped glomeruli. However, we found that MGC 1 is a part of the toroid (MGC 3). It is a protuberant structure rising dorsally into the cumulus (MGC 2) from a posterior part of the toroid—MGC 3 (Figures 1C and 8). This is supported by the morphological structure of the toroid-PNs characterized in this study (e.g. Figures 7 and 8). Most of the toroid-PNs, constituent neurons of the toroid, had

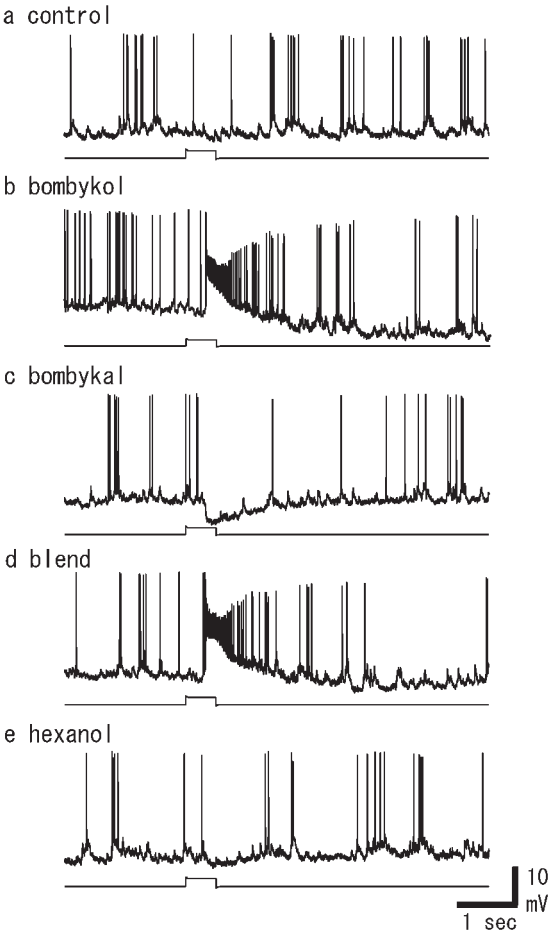

branchings with tufts in the medio-dorsal part of the MGC (Figure 8A–D, thick arrows), which corresponds to a protuberant structure rising dorsally into the cumulus from a posterior part of the toroid (Figure 1C). Moreover, projection patterns of some types of antennal sensory fibers restricted to MGC 1 and 3 were observed by cobalt staining from cut hairs on the antenna (Koontz and Schneider, 1987). Judging from our physiological results, that toroid-PNs respond exclusively to bombykol, these sensory fibers may carry bombykol information to the toroid including the protuberant structure.

MGC-projection neurons

In *M. sexta* MGC-PNs, the pheromone blend or a component of the pheromone evokes a characteristic triphasic response consisting of a brief, hyperpolarizing inhibitory potential followed by depolarization with firing of action potentials and then a delayed period of hyperpolarization (Christensen and Hildebrand, 1987; Hansson and Christensen, 1999). In contrast, *B. mori* MGC-PNs showed a biphasic response to pheromonal stimulation; typically the

Figure 11 Physiological profile of the toroid-PN shown in Figure 7A. Responses to antennal stimulation with two pheromone components and hexanol. The cell showed excitatory responses to bombykol and blend, and inhibitory responses to bombykal. Hexanol and control did not elicit any responses. Another two sets of olfactory stimulation showed similar response patterns.

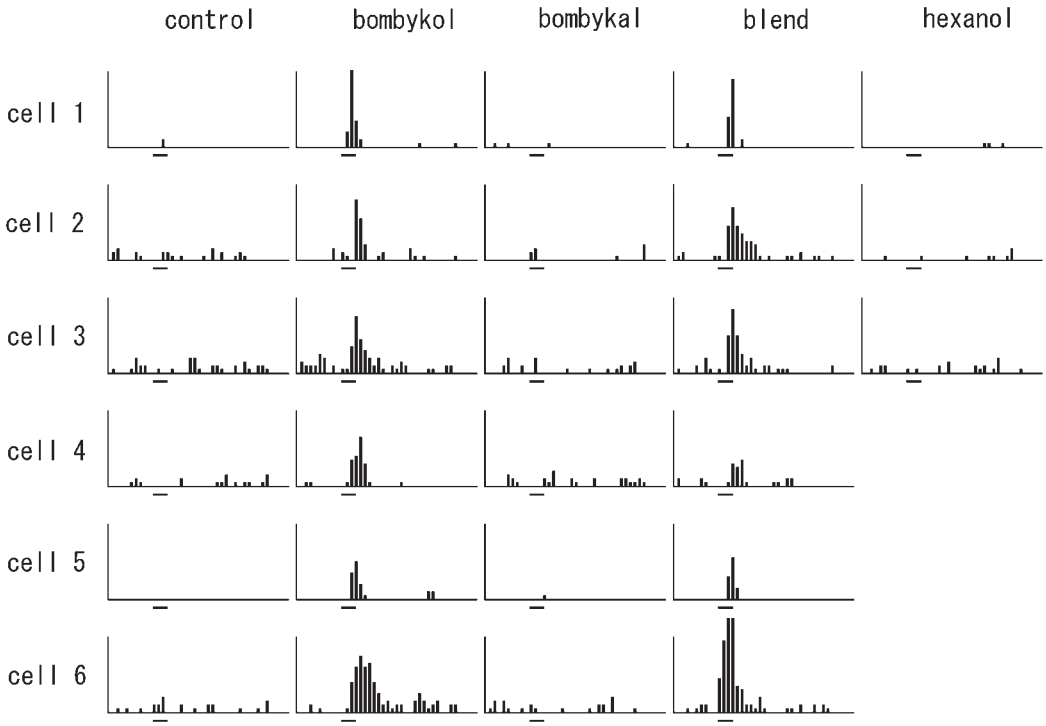

Figure 12 Spike frequency histograms for toroid-PNs. All the toroid-PNs tested selectively responded to bombykol and blend with excitation; *x*-axis = 0–7 s, stimulus marker = 0.5 s; *y*-axis = 0–20 spikes/0.2 s bin.

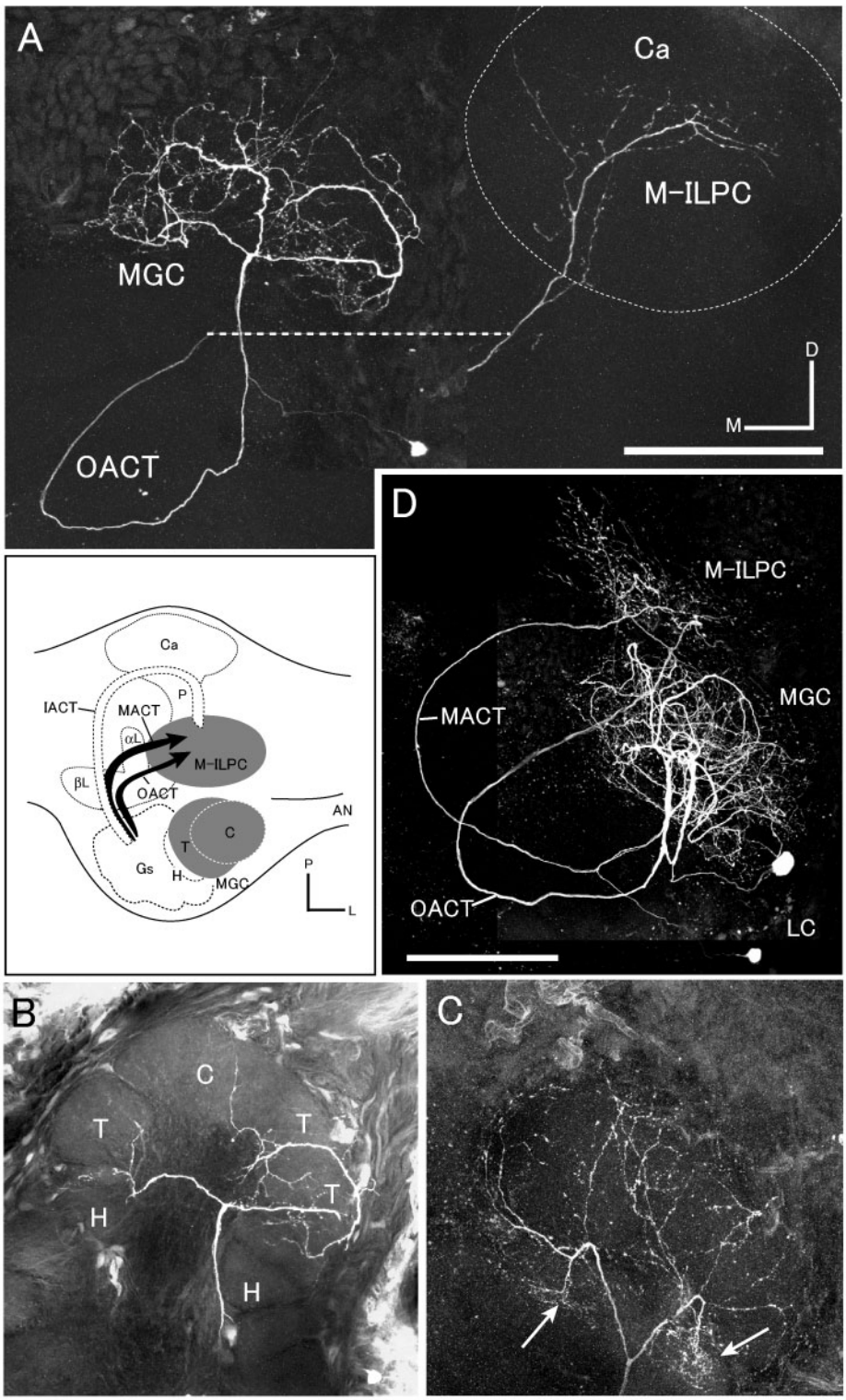

Figure 13 Morphology of c + t-PNs. **(A)** This cell has dendritic arborizations in both the cumulus and toroid with fine spines and its cell body in the LC. The axon passes through the OACT and sends blebby terminals extending to the medial part of the ILPC (M-ILPC). No branches were observed in the Ca. Frontal view. The dashed line links processes that were separated to reveal the structures of branches that overlapped *in situ*. **(B)** Confocal slice images of A in the MGC. Both the cumulus and toroid are invaded by fine processes with spines. **(C)** The c + t PN has dendritic arborizations in both the cumulus and toroid. Some branches are also observed in the horseshoe (arrows). The cell has its cell body in the LC and its axon runs in the MACT (not shown). Scale bar in A for A, B and C = 100 μm. **(D)** Two c + t PNs were simultaneously stained in a brain. Both have cell bodies in the LC. One axon is in the MACT and other in the OACT. Both PNs send projections into the M-ILPC, but not into the Ca. Scale bar = 100 μm. Inset is a schematic drawing of the hemisphere of the brain showing projection sites of the cells.

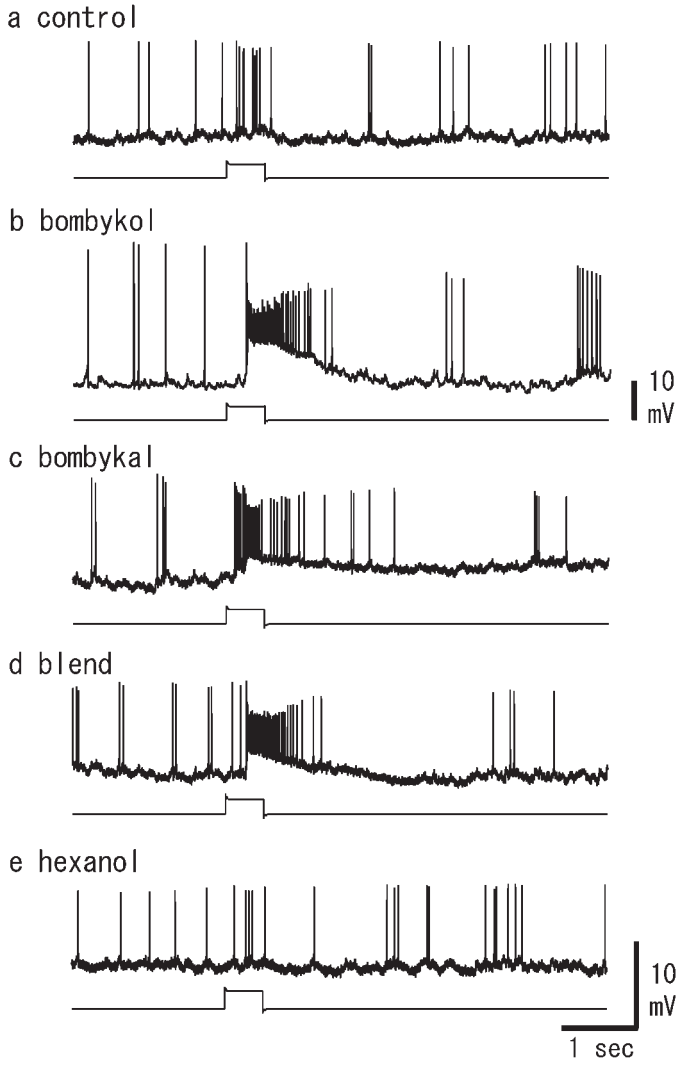

Figure 14 Physiological profile of a c + t-PN. Responses to antennal stimulation with two pheromone components and hexanol. The cell showed excitatory responses to bombykol, bombykal and blend. Hexanol and control elicited slight excitatory responses, suggesting a weak mechanosensory response. Another two sets of olfactory stimulation showed similar response patterns.

firing of action potentials followed by a period of hyperpolarization. Initial hyperpolarizing inhibition was not observed (Figures 5, 10, 11, 14 and 16). Similar response characteristics to *B. mori* were reported in MGC-PNs of the noctuids *H. virescens* and *H. zea* (Vickers *et al.*, 1998; Hansson and Christensen, 1999).

It has been reported that *M. sexta* males have ~30 MGC-PNs, based on numerical comparison of cells in the ALs of male and female moths using anatomical techniques (Homberg *et al.*, 1988). Since the total number of cell bodies contained in the MC is almost the same in *M. sexta* and *B. mori*—~200 (Homberg *et al.*, 1988; Seki and Kanzaki, 2002)—*B. mori* males are also thought to have similar number of MGC-PNs. In the present study we have characterized morphologically and/or physiologically 37 MGC-PNs in *B. mori* males. These MGC-PNs were classified into four groups according to the branching areas of dendritic arborizations in the subdivisions of the MGC: cumulus-PNs; toroid-PNs; cumulus and toroid-PNs (c + t-PNs); and horseshoe-PNs (Table 1).

In general, MGC-PNs that responded exclusively to bombykol (the principal component of the pheromone blend) had arborizations confined to the toroid, including a protuberant structure rising dorsally into the cumulus from a posterior part of the toroid (Figures 7, 8 and 10–12). Whereas PNs that responded selectively to bombykal (the minor pheromone component) had arborizations within the cumulus (Figures 2, 3, 5 and 6) or the horseshoe (Figures 15and 16). In this study we present the first report of morphological and/or physiological properties of horseshoe-PNs in moths. A horseshoe-PN showed excitatory responses selectively to bombykal (Figure 16).

PNs that showed excitatory responses to both pheromone components had arborizations in both the cumulus and toroid (c + t-PNs; Figure 14). One c + t-PN had fine branches in the horseshoe as well (Figure 13C). This is interesting because we found a horseshoe-PN which showed excitatory responses to bombykal. It is a possibility that the c + t-PN may receive bombykal information not only in the cumulus but also in the horseshoe. These results indicate that information about these two pheromone components is processed initially in different regions of the MGC.

In two of the toroid-PNs bombykol and bombykal elicited excitatory and inhibitory responses, respectively. These PNs perform a higher level of processing than other PNs that arborize in the same subdivisions. Similar responses have been reported in PNs of *M. sexta* (Christensen and Hildebrand, 1987) and *H. virescens* (Christensen *et al.*, 1995, Mustaparta, 1996). In the present study, c + t-PNs had cell bodies in the LC in the AL and axons in the MACT or OACT (Table 1 and Figure 13). We previously reported that the c + t-PNs showed dose–response characteristics (Kanzaki and Shibuya, 1986). *M. sexta* PNs which have cell bodies in the LC have been reported, but which ACT their axons pass through is not known (Heinbockel *et al.*, 1998).

We found toroid-PNs which have distinct tufts in a variety of confined regions in the toroid (Figure 8). Koontz and Schneider (Koontz and Schneider, 1987) reported that the terminal arborizations of all olfactory receptor neurons (ORNs) in the MGC are confined to a region ~50 μm in diameter in the MGC. Most of the PNs characterized in the study had arborizations separated into some distinct tufts in the toroid within ~50 μm (Figure 8). The diameter of these arborizations corresponds to that of the terminal region of ORNs. Such a confined field size suggests the possibility that different ORN types may be segregated into different distinct tufts of PNs. Local interneurons and feedback neurons from the PC also have their arborizations in this

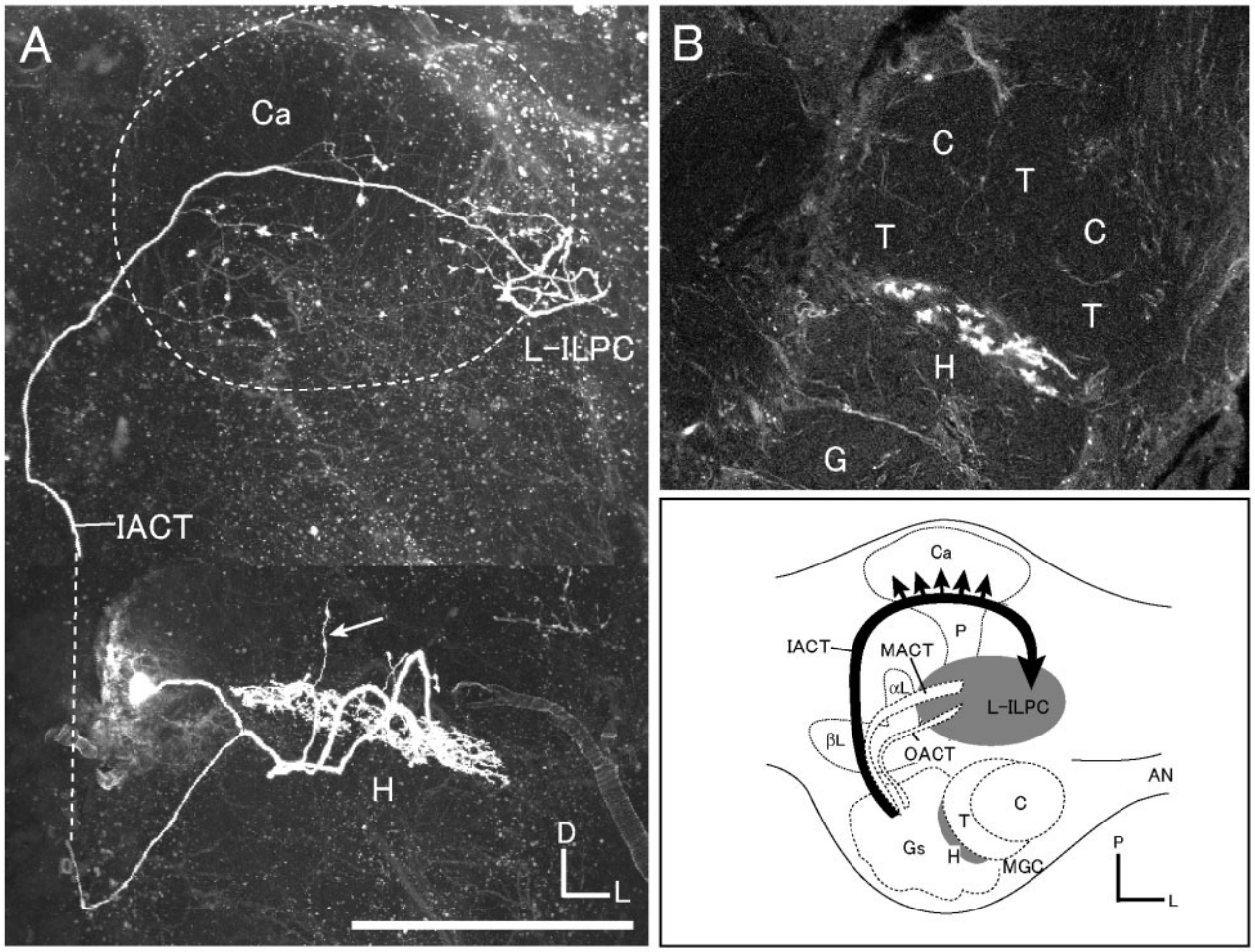

Figure 15 Morphology of a horseshoe-PN. **(A)** Dendritic arborizations are restricted to the horseshoe (H). Short profiles (arrow) projecting to the coarse fiber area in the center of the MGC. The cell body is in the MC. The axon runs in the IACT and sends blebby branchings to Ca and the lateral part of the ILPC (L-ILPC). **(B)** Confocal slice image of the MGC of A. The branching region of the PN is restricted to the horseshoe (H). Frontal view. Scale bar = 100 μm. Inset is a schematic drawing of the hemisphere of the brain showing projection sites of the cell.

field (Hill *et al.*, 2002; Seki and Kanzaki, 2002). It seems that this confined field may play a role as a local circuit for olfactory coding. Further, it is possible that there is a functional connection between the toroid and cumulus. In the present study, two toroid-PNs showed excitatory responses to the major pheromone component, bombykol, and inhibitory responses to the minor component, bombykal (Figure 11). There may be some connections between the cumulus and toroid, possibly mediated by some GABAergic local interneurons (Christensen *et al.*, 1998). In *M. sexta*, indirect routes of excitatory input to PNs via intercalated excitatory interneurons (Sun *et al.*, 1997) or through disinhibitory circuits involving two inhibitory interneurons arranged in series have been found (Distler and Boeckh, 1997a, b; Christensen *et al.*, 1998).

None of the MGC-PNs tested (n = 12) in this study responded to 1-hexanol. Although we must investigate responsiveness to many other non-pheromonal odors, as reported in some species of moths, *B. mori* MGC-PNs may also be specialized only for pheromone processing (Hansson and Christensen, 1999).

Projections in the calyces of the mushroom body and the lateral protocerebrum

MGC-PNs transfer pheromonal information to higher olfactory centers in the PC, including the Ca and the ILPC through the antennocerebral tracts (ACTs). In *M. sexta* five different ACTs have been reported: inner (IACT), medial (MACT), outer (OACT), dorsal (DACT) and dorsolateral ACTs (DLACT) (Homberg *et al.*, 1988). Most of the physiologically characterized MGC-PNs of *M. sexta* run through the IACT (Hansson *et al.*, 1991; Hansson and Christensen, 1999). Besides the IACT pathways, cobalt injection into the MGC of *M. sexta* revealed that some MGC-PNs have axonal pathways in the OACT and MACT (Homberg *et al.* 1988; Kanzaki *et al.*, 1989). However, physiological and morphological properties of *M. sexta* MGC-PNs which pass through the OACT or MACT have

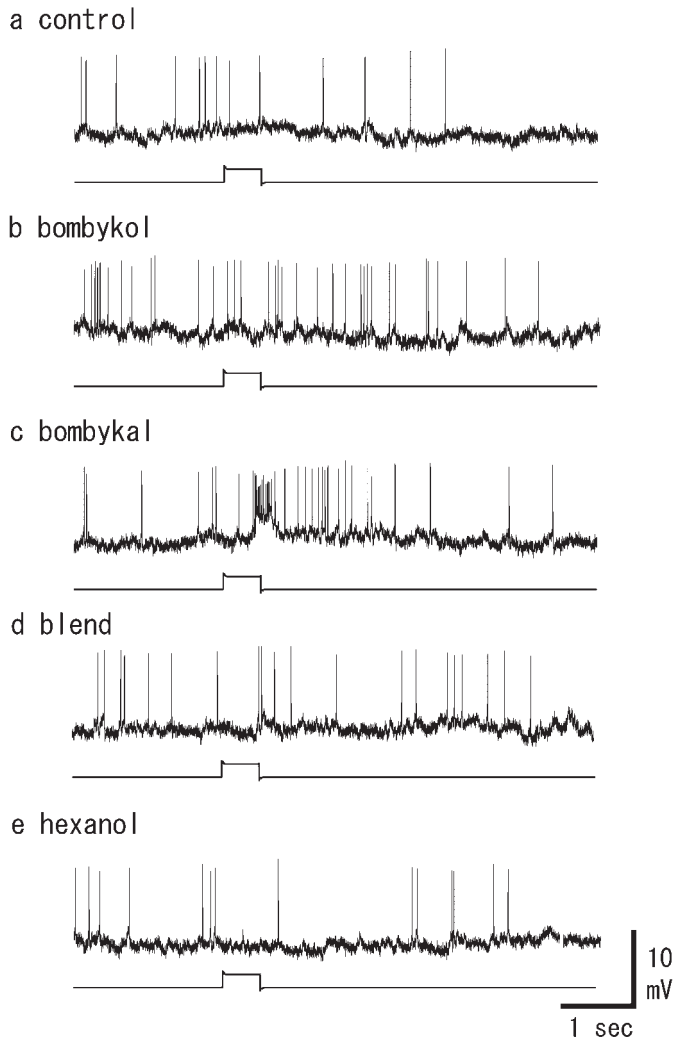

Figure 16 Physiological profile of a horseshoe-PN. Responses to antennal stimulation with two pheromone components and hexanol. The cell showed excitatory responses to bombykal. Bombykol, mixture, hexanol and control did not elicit any responses. Another two sets of olfactory stimulation showed similar response patterns.

not yet been well characterized. In the present study, we physiologically and/or morphologically characterized *B. mori* MGC-PNs which take three different pathways to the PC: IACT (n = 31), MACT (n = 3) and OACT (n = 3) (Table 1).

All the cumulus-PNs, toroid-PNs and horseshoe-PNs characterized in this study had their cell bodies in the MC of the AL and passed through the IACT to the PC including the Ca and the ILPC. Interestingly, the projection patterns and areas in the Ca and the ILPC were different between the cumulus- and horseshoe-PNs, and the toroid-PNs (Table 1). The axons of the cumulus- and horseshoe-PNs sent blebby axonal branches into the whole Ca and extended branchings with blebby terminals to a small field in the lateral part of the ILPC (Figures 2, 4 and 15). However, toroid-PNs sent only a single or a few short blebby branches into the Ca and extended wide-field branchings with blebby terminals to the medial part of the ILPC (Figures 7 and 9). Two toroid-PNs which had dendritic arborizations with numerous fine spines sent wide-field thick blebby branches extending into the medial part of the ILPC bypassing the Ca (Figure 7B and Table 1). Cumulus- and horseshoe- and toroid-PNs showed excitatory responses selectively to bombykal and bombykol, respectively. These results suggest that information about each pheromone component is conserved at the level of the Ca and the ILPC, and it seems that the Ca may not be a prominent processing site for the major pheromone component, bombykol. The Ca may be instead a processing site for minor pheromonal information and non-pheromonal information. We have characterized some ordinary glomerular PNs, whose axons sent dense blebby branches into the whole calyces (data not shown). In contrast, all the characterized types of *M. sexta* PNs (cumulus- and toroid-PNs) which transfer pheromone information, have prominent branchings with varicosities clustered in certain areas of the Ca (Homberg *et al.*, 1988; Hansson *et al.*, 1991). While, it is generally accepted that the Ca and the ILPC are the target sites for olfactory information from the MGC in moths, our results suggest that the ILPC, especially the medial part of the ILPC may be the more important processing site for major pheromonal information in *B. mori*.

Physiological, behavioral and genetic studies in several insect species suggest that the MB is critical for olfactory and other forms of associative memory (Heisenberg, 1998; De Belle and Kanzaki, 1999). In *B. mori* the major pheromone component, bombykol is sufficient to release the complete odor modulated behavior (Kanzaki, 1998). It is interesting that toroid-PNs which selectively transfer bombykol information to the PC had major projections to the ILPC, especially to the medial part of the ILPC but not to the Ca. This suggests that the bombykol-driven behavior of *B. mori* may be an independent behavior isolated from olfactory associative memory.

In the present study we revealed the projection sites of horseshoe-PNs. They had projections into the Ca and the lateral part of the ILPC through the IACT. These morphological properties are similar to those of cumulus-PNs. Interestingly, the physiologically characterized horseshoe-PN in this study also showed similar response characteristics to those of cumulus-PNs, that is, the cell responded selectively to bombykal.

In the present study we morphologically and/or physiologically characterized c + t-PNs (n = 6). The c + t-PN tested showed excitatory responses to both bombykol and bombykal (Figure 14). These c + t-PNs are morphologically different from toroid-PNs and cumulus-PNs in the following three points (Table 1): (i) all of these c + t-PNs had their cell bodies in the LC instead of the MC; (ii) all of these c + t-PNs passed through the MACT or the OACT to ILPC instead of the IACT; and (iii) all these c + t-PNs projected only to the ILPC, bypassing the Ca (e.g. Figure 13D).

Although the paths to the ILPC are different, i.e. MACT or OACT, it seems that the projection areas of these two types of c + t-PNs overlap in the ILPC. However, we still do not know whether the projection areas of c + t-PNs overlap with those of toroid-PNs, cumulus-PNs and horseshoe-PNs. Multiple staining of these PNs in the same brain is our ongoing work in order to investigate precise target areas of these PNs running through each pathway to the ILPC, which will lead to some important advances in understanding the processing of pheromone information in a higher olfactory center, the ILPC.

Acknowledgements

The authors thank Dr Evan Hill for his critical comments on the manuscript. This research was supported by a grant from the basic research activities for innovative bioscience (BRAIN) and a grant-in-aid for scientific research on priority area (A) from the Ministry of Education, Culture, Sports, Science and Technology of Japan (11168207).

References

Boeckh, J. and **Boeckh, V.** (1979) *Threshold and odor specificity of pheromone-sensitive neurons in the deutocerebrum of* Antheraea pernyi *and* A. polyphemus (*Saturniidae*). J. Comp. Physiol. A, 132, 235–242.

Boeckh, J. and **Tolbert, L.P.** (1993) *Synaptic organization and development of the antennal lobe in insects.* Microsc. Res. Tech., 24, 260–280.

Butenandt, A., **Beckermann, R.**, **Stamm, D.** and **Hecker, E.** (1949) *Über den Sexuallockstoff des Seidenspinners* Bombyx mori*. Reindarstellung udn Konstitution.* Z. Naturforsch., 14b, 283–284.

Christensen, T.A. and **Hildebrand, J.G.** (1987) *Male-specific, sex pheromone-selective projection neurons in the antennal lobes of the moth* Manduca sexta*.* J. Comp. Physiol. A, 160, 553–569.

Christensen, T.A. and **Hildebrand, J.G.** (1996) *Coincident stimulation with pheromone components improves temporal pattern resolution in central olfactory neurons*. J. Neurophysiol., 77, 775–781.

Christensen, T.A. and **White, J.** (2000) *Representation of olfactory information in the brain.* In Finger, T.E., Silver, W.L. and Restrepo, D. (eds), The Neurobiology of Taste and Smell, 2nd edn. Wiley-Liss, New York, pp. 201–232.

Christensen, T.A., Mustaparta, H. and **Hildeband, J.G.** (1995) *Chemical communication in heliothine moths. VI. Parallel pathways for information processing in the macroglomerular complex of the male tobacco budworm moth* Heliothis virescens. J. Comp. Physiol. A., 177, 545–557.

Christensen, T.A., Waldrop, B.R. and **Hildebrand, J.G.** (1998) *Multitasking in the olfactory system: context-dependent responses to odors reveal dual BABA-regulated coding mechanisms in single olfactory projection neurons*. J. Neuroscience, 18, 5999–6008.

De Belle, J.S. and **Kanzaki, R.** (1999) *Protocerebral olfactory processing.* In Hansson, B.S. (ed.), Insect Olfaction. Springer, Berlin, pp. 125–161.

Distler, P.G. and **Boeckh, J.** (1997a) *Synaptic connection between identified neuron types in the antennal lobe glomeruli of the cockroach,* Periplaneta americana*. I. Uniglomerular projection neurons*. J. Comp. Neurol., 378, 307–319.

Distler, P.G. and **Boeckh, J.** (1997b) *Synaptic connection between identified neuron types in the antennal lobe glomeruli of the cockroach,* Periplaneta americana*. II. Local multiglomerular interneurons*. J. Comp. Nerol., 383, 529–540.

Hansson, B.S. and **Christensen, T.A.** (1999) *Functional characteristics of the antennal lobe.* In Hansson, B.S. (ed.), Insect Olfaction. Springer, Berlin, pp. 125–161.

Hansson, B.S., Christensen, T.A. and **Hildebrand, J.G.** (1991) *Functionally distinct subdivisions of the macroglomerular complex in the antennal lobe of the male sphinx moth* Manduca sexta*.* J. Comp. Neurol., 312, 264–278.

Heinbockel, T., Kloppenburg, P. and **Hildebrand, J.G.** (1998) *Pheromone-evoked potentials and oscillations in the antennal lobes of the sphinx moth* Manduca sexta*.* J. Comp. Physiol. A, 182, 703–714.

Heisenberg, M. (1998) *What do the mushroom bodies do for the insect brain? An introduction*. Learn. Mem., 5, 1–10.

Hildebrand, J.G. (1996) *Olfactory control of behavior in moths: central processing of odor information and the functional significance of olfactory glomeruli*. J. Comp. Physiol. A, 178, 5–19.

Hildebrand, J.G. and **Shepherd, G.M.** (1997) *Mechanisms of olfactory discrimination: converging evidence for common principles across phyla*. Annu. Rev. Neurosci., 20, 595–631.

Hill, E.S., Iwano, M., Gatellier, L. and **Kanzaki, R.** (2002) *Morphology and physiology of the serotonin-immunoreactive putative antennal lobe feedback neuron in the male silkmoth* Bombyx mori. Chem. Senses., 27, 475–483.

Homberg, U., Montague, R.A. and **Hildebrand, J.G.** (1988) *Anatomy of antenno-cerebral pathways in the brain of the sphinx moth* Manduca sexta*.* Cell Tissue Res., 254, 255–281.

Kaissling, K-E. and **Kasang, G.** (1978) *A new pheromone of the silkworm moth* Bombyx mori. Naturewissenschaften, 65, 382–384.

Kaissling, K.-E. and **Priesner, E.** (1970) *Die Riechswelle des Seidenspinners.* Naturwissenschaften, 57, 23–28.

Kanzaki, R. (1998) *Coordination of wing motion and walking suggests common control of zigzag motor program in a male silkworm moth*. J. Comp. Physiol. A, 182, 267–276.

Kanzaki, R. and **Shibuya, T.** (1983) *Olfactory neural pathway and sexual pheromone responses in the deutocerebrum of the male silkworm moth,* Bombyx *mori (Lepidoptera: Bombycidae).* Appl. Ent. Zool., 18, 131–133.

Kanzaki, R. and **Shibuya, T.** (1986) *Identification of the deutocerebral neurons responding to the sexual pheromone in the male silkworm moth brain*. Zool. Sci., 3, 409–418.

Kanzaki, R., Arbas, E.A., Strausfeld, N.J. and **Hildebrand, J.G.** (1989) *Physiology and morphology of projection neurons in the antennal lobe of the male moth* Manduca sexta*.* J. Comp. Physiol. A, 165, 427–453.

Kanzaki, R., Ikeda, A. and **Shibuya, T.** (1994) *Morphological and physiological properties of pheromone-triggered flipflopping descending interneurons of the male silkworm moth,* Bombyx mori. J. Comp. Physiol. A, 175, 1–14.

Koontz, M.A. and S**chneider, D.** (1987) *Sexual dimorphisms in neuronal projections from the antennae of silk moths (*Bombyx mori*,* Antheraea polyphemus*) and the gypsy moth (*Lymantria dispar*).* Cell Tissue Res., 249, 39–50.

Matsumoto, S.G. and **Hildebrand, J.G.** (1981) *Olfactory mechanisms in the moth* Manduca sexta*: response characteristics and morphology of central neurons in the antennal lobes*. Proc. R. Soc. Lond. B, 213, 249–277.

Mishima, T. and **Kanzaki, R.** (1999) *Physiology and morphology of*

olfactory descending interneurons of the male silkworm moth, Bombyx mori. J. Comp. Physiol. A, 184, 143–160.

Mustaparta, H. (1996) *Central mechanisms of pheromone information processing*. Chem. Senses, 21, 269–275.

Seki, Y. and **Kanzaki, R.** (2002) *Classification of the local interneurons in the antennal lobe of the silkmoth* Bombyx mori. Zool. Sci. Abstr., in press.

Soo, K. and **Kanzaki, R.** (2000) *Identification of glomerular structures in the antennal lobe of* Bombyx mori. Zool. Sci. Abstr., 17, 108.

Strausfeld, N.J. (1989) *Cellular organization in male-specific olfactory neuropil in the moth* Manduca sexta. In Elsner, N. and Singer, W. (eds), Dynamics and Plasticity in Neuronal Systems. Thieme, Stuttgart, abstr. 79.

Sun, X.J., Tolbert, L.P. and **Hildebrand, J.G.** (1997) *Synaptic organization of the uniglomerular projection neurons of the antennal lobe of the moth* Manduca sexta*: a laser scanning confocal and electron microscopic study*. J. Comp. Neurol., 379, 2–20.

Vickers, N.J., Christensen, T.A. and **Hildebrand, J.G.** (1998) *Combinatorial odor discrimination in the brain: attractive and antagonist odor blends are represented in distinct combinations of uniquely identifiable glomeruli*. J. Comp. Neurol., 400, 35–56.

Accepted November 28, 2002